The Journal of Experimental Biology 204, 959–966 (2001)
Printed in Great Britain © The Company of Biologists Limited 2001
JEB2922

NOVEL SUBCELLULAR AND MOLECULAR TOOLS TO STUDY Ca^{2+} TRANSPORT MECHANISMS DURING THE ELUSIVE MOULTING STAGES OF CRUSTACEANS: FLOW CYTOMETRY AND POLYCLONAL ANTIBODIES

MICHELE G. WHEATLY*, ZHIPING ZHANG, JENNIFER R. WEIL, JAMES V. ROGERS AND LA'TONIA M. STINER

Department of Biological Sciences, Wright State University, Dayton, OH 45435, USA

*e-mail: michele.wheatly@wright.edu

Accepted 1 December 2000; published on WWW 12 February 2001

Summary

Our understanding of calcium homeostasis during the crustacean moulting cycle derives from research on intermoult animals that has been extrapolated to other stages. In terms of transepithelial Ca^{2+} flux, the more interesting stages are those surrounding ecdysis since crustaceans experience a sizeable negative calcium balance in immediate premoult and a significant positive calcium balance in immediate postmoult. These stages are elusive in the sense that larger species such as lobsters are rarely captured at this time, and smaller species such as blue crabs and crayfish are seldom synchronized in their moulting cycle. The reductionist approaches employed in cellular physiology, such as vesicle techniques, employ pooling of fresh tissues from many organisms. Examination of the elusive moulting stages requires more sensitive approaches that can utilize tissue from an individual crustacean to characterize Ca^{2+} pumps (*S*arco/*E*ndoplasmic *R*eticulum *C*a^{2+}-*A*TPase, SERCA; *P*lasma *M*embrane *C*a^{2+}-*A*TPase, PMCA) and the *N*a^{+}/*C*a^{2+} e*X*changer (NCX). An emerging subcellular approach described in this paper is to use flow cytometry as a technique to monitor Ca^{2+} uptake into Fluo-3-loaded membrane vesicles. This paper illustrates the utility of this technique for measuring ATP-dependent Ca^{2+} uptake into hepatopancreatic basolateral membrane vesicles. Obstacles to progress in molecular studies have not been limited by synchronization of moulting since tissue can be snap-frozen and collected from many animals over time. Here, the problem has been the lack of specific antibodies that hybridize with the Ca^{2+} transporters of interest so that they can be localized within epithelia. In this paper, we introduce polyclonal antibodies raised in rabbits against crayfish SERCA, PMCA and NCX. Immunocytochemistry of SERCA in muscle, PMCA in antennal gland and NCX in heart confirms the specificity of the antibodies.

Key words: crayfish, *Procambarus clarkii*, flow cytometry, sarco/endoplasmic reticulum Ca^{2+}-ATPase, plasma membrane Ca^{2+}-ATPase, Na^{+}/Ca^{2+} exchanger, polyclonal antibody.

Introduction

In the 1970–1980s, decapod crustaceans became popular invertebrate models for the study of respiratory gas exchange and acid–base balance (McMahon and Wilkens, 1983; Truchot, 1983). Their unique moulting cycle became a focus for integrative crustacean biology (Mangum et al., 1985) especially in the context of the effects of calcification/decalcification on calcium and CO_2 homeostasis (Cameron and Wood, 1985). Our laboratory has built on these early studies to develop the moulting cycle of the freshwater crayfish *Procambarus clarkii* as a model for transepithelial Ca^{2+} translocation and subcellular homeostasis and for the regulation of the expression of genes encoding Ca^{2+}-translocating proteins (Wheatly, 1996, 1997, 1999). The beauty of this model system is that $[Ca^{2+}]$ is regulated spatially and temporally. Free Ca^{2+} levels may be simultaneously high at calcification/storage sites and low in the cytosol. Net transepithelial Ca^{2+} movement, which is virtually negligible in intermoult crayfish (Ca^{2+} balance), cycles through net efflux in premoult and becomes a net influx in postmoult animals. For the crayfish, the problem of Ca^{2+} homeostasis is acute since it resides in a calcium-deficient environment ($<1\ mmol\ l^{-1}$). Research on mechanisms of crustacean Ca^{2+} homeostasis over the past 15 years has focused on intermoult crustaceans. This review will outline novel subcellular and molecular approaches that will be required to explore calcium homeostasis fully in the more elusive pre- and postmoult stages.

Novel subcellular approaches

Background and obstacles for elusive moulting stages

The subcellular model for crustacean Ca^{2+} homeostasis has been based on *in vitro* vesicle studies performed on intermoult

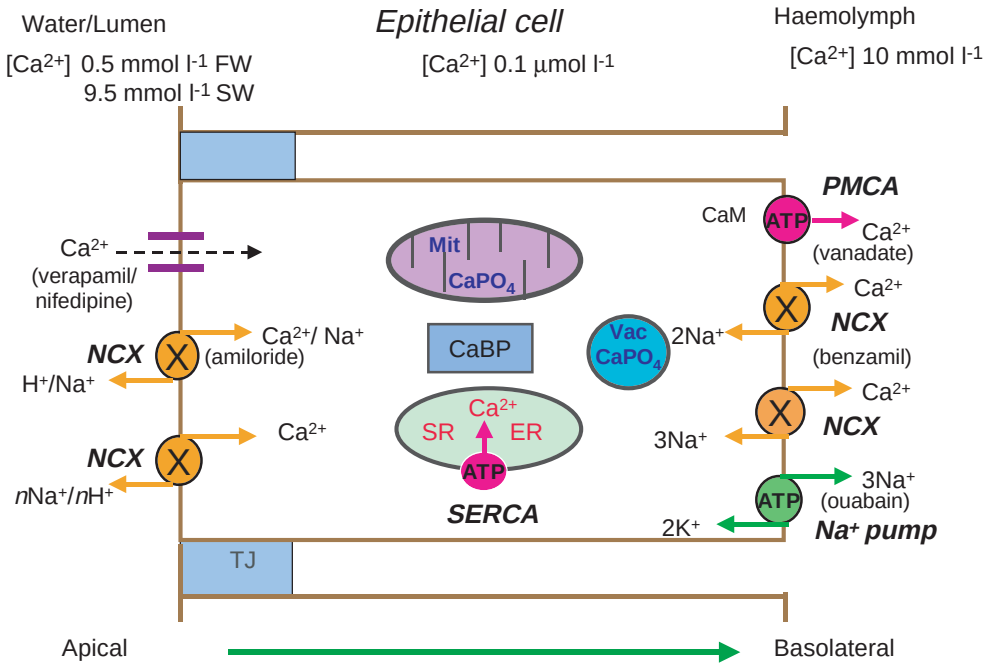

Fig. 1. A working model for apical-to-basolateral transcellular Ca^{2+} transport in crustacean epithelial cells (gills, antennal gland, hepatopancreas) based on studies using isolated membrane vesicles. Pharmaceutical inhibitors are shown in parentheses. SR, sarcoplasmic reticulum; ER, endoplasmic reticulum; CaBP, Ca^{2+}-binding protein; TJ, tight junction; CaM, calmodulin; Mit, mitochondria; Vac, vacuole; FW, fresh water; SW, sea water; NCX, Na^+/Ca^{2+} exchanger; SERCA, sarco/endoplasmic reticulum Ca^{2+}-ATPase; PMCA, plasma membrane Ca^{2+}-ATPase; $CaPO_4$, calcium phosphate.

animals and extrapolated to other moulting stages. Species studied include the marine lobster *Homarus americanus* (hepatopancreas, a liver analogue and antennal gland, a kidney analogue; Ahearn and Franco, 1993; Ahearn and Zhuang, 1996; Zhuang and Ahearn, 1996, 1998), the shore crab *Carcinus maenas* (gill; Flik et al., 1994) and the freshwater crayfish *Procambarus clarkii* (gill, antennal gland, hepatopancreas; Wheatly et al., 1998, 1999; M. G. Hubbard and M. G. Wheatly, unpublished data). The generally accepted model for unidirectional apical-to-basolateral influx (as exemplified in postmoult gill and hepatopancreas, premoult hypodermis and intermoult antennal gland, see Fig. 1) is that Ca^{2+} enters the apical membrane passively through carrier-mediated facilitated diffusion, through a Ca^{2+}/nNa^+ (or H^+) antiporter that may be electroneutral or electrogenic, or *via* simple diffusion through verapamil- or nifedipine-inhibited potential-difference-dependent Ca^{2+} channels. Active basolateral efflux involves a vanadate-sensitive high-affinity but low-capacity calmodulin-dependent plasma membrane Ca^{2+}-ATPase (PMCA, K_m 0.1–0.2 µmol l^{-1}, J_{max} <1 nmol mg^{-1} min^{-1} in tissues of freshwater crustaceans, 10–100 nmol mg^{-1} min^{-1} in tissues of marine crustaceans) and a low-affinity, high-capacity Na^+/Ca^{2+} exchanger (NCX) whose activity is fuelled by the Na^+ pump. The NCX characterized in crayfish hepatopancreas and antennal gland and in crab gill appears to be electroneutral (K_m 1–2 µmol l^{-1}, J_{max} 2–20 nmol mg^{-1} min^{-1}). However, kinetic experiments in lobster hepatopancreas reveal a K_m of 15 µmol l^{-1} and a J_{max} of 50–600 nmol mg^{-1} min^{-1} for an exchanger that is purportedly electrogenic ($Ca^{2+}/3Na^+$; Zhuang and Ahearn, 1998). Collectively, these studies suggest the presence of two different NCXs on the basolateral membrane, as on the apical membrane. Intermoult kinetic experiments have suggested that the PMCA serves a 'housekeeping' role in regulating intracellular $[Ca^{2+}]$, while the NCX is the 'workhorse' primarily responsible for basolateral Ca^{2+} efflux. Net unidirectional basolateral-to-apical Ca^{2+} efflux (as exemplified in premoult hepatopancreas and postmoult hypodermis) repositions active processes such as the Ca^{2+} pump on the apical membrane (Greenaway et al., 1995).

While *en route* through the epithelial cell, intracellular Ca^{2+} can be sequestered in organelles such as the sarco/endoplasmic reticulum or mitochondria. Sarco/endoplasmic reticulum Ca^{2+}-ATPase (SERCA) pumps have been characterized in purified muscle sarcoplasmic reticulum from intermoult *Procambarus clarkii* and *Potamon potamios*; SERCA tends to have a lower affinity but higher capacity than PMCA, commensurate with its relative abundance (Wheatly, 1999). In crustaceans, differential mitochondrial Ca^{2+} transport/storage throughout the moulting cycle has been studied in lobster hepatopancreas (Klein and Ahearn, 1999) and crayfish antennal gland (Rogers and Wheatly, 1997). Hepatopancreatic transmitochondrial flux was elevated in the premoult stage when calcium removed from the cuticle entered the gut for storage between moults. Renal mitochondrial storage was elevated during postmoult associated with maximal calcium reabsorption. Intracellular calcium can also be bound to protein or concealed in membrane-clad vesicles.

Applying established vesicle techniques to pre- and postmoult crustaceans has been impossible because of the logistical difficulty of obtaining sufficient tissue samples in those stages. For example, crayfish tissue must be pooled from 6–10 medium-sized animals to detect uptake of $^{45}Ca^{2+}$ into filtered vesicles (this is especially true of antennal glands, which together weigh less than 0.1 g). To employ this technique in the study of pre- or postmoult animals, it would

be necessary to synchronize ecdysis precisely in many crayfish. Research on moulting stages has employed artificial means (multiple limb autotomy or removal of the eyestalks, which contain the X-organ/sinus gland axis) to precipitate ecdysis. Even these tactics do not guarantee synchronization to the day of ecdysis let alone the hour. For Ca^{2+} homeostasis, the time line is important since Ca^{2+} flux dynamics can alter drastically in a matter of hours. Furthermore, work in our laboratory has shown that crayfish undergoing forced moults are not physiologically equivalent to those moulting naturally (Wheatly and Hart, 1995). We therefore abandoned the idea of synchronizing ecdysis in multiple crayfish in favour of developing a more sensitive method to detect Ca^{2+} uptake into vesicles from individual crayfish. A promising emerging technology is the use of flow cytometry to detect Ca^{2+} uptake into Fluo-3-loaded vesicles.

Flow cytometry as a more sensitive method to detect Ca^{2+} uptake into Fluo-3-loaded vesicles

Traditionally, flow cytometry has been used as a clinical tool for studying properties of individual intact cells such as size, surface antigen, protein/DNA/RNA content, Ca^{2+} influx and pH. In this technique, quantitative information is based on light scattering or fluorescence emission caused by individual cells in a population as they flow rapidly in a fluid stream in front of a light source. Recently, this technology has been extended through analysis of small particles to subcellular fractions (<1 μm diameter) such as liposomes, endosomes, platelets, lymphocytes and membrane vesicles. Because of the reduction in particle size, orthogonal (90 °) side scatter becomes increasingly useful in determining the characteristics of subcellular particles.

Two studies have conclusively demonstrated that flow cytometry analysis represents a useful tool for quantifying the kinetics and pharmacology of the putative Ca^{2+}-translocating proteins in mammalian membrane vesicles. Ishida and Chused (1988) used flow cytometry to measure Ca^{2+} influx into mouse B and T lymphocyte vesicles loaded with the Ca^{2+} chelator Indo-1. Subsequently, Telford and Miller (1996) modified that original method by isolating inside-out vesicles of mouse T lymphocytes and loading them with the fluorescent Ca^{2+}-chelating dye Fluo-3. In both studies, inside-out vesicles appeared as a subpopulation of low-forward-scatter/low-side-scatter events that could be distinguished from higher-side-scatter debris. In both these earlier studies, an increase in fluorescence was observed in dye-loaded vesicles treated with

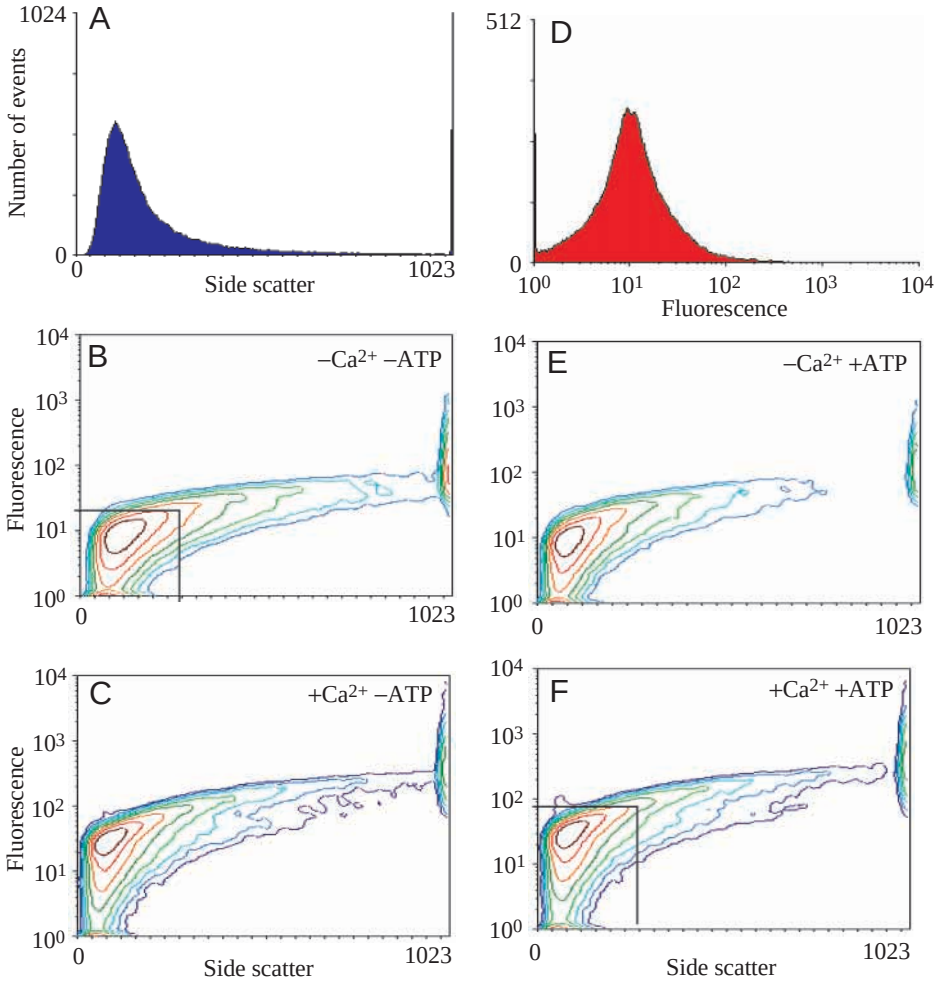

Fig. 2. Representative data gathered using flow cytometry to measure Ca^{2+} fluorescence of Fluo-3-loaded basolateral membrane vesicles (BLMVs) in the presence (+) and absence (–) of Ca^{2+} and ATP. A plot of the number of events *versus* 90 ° side-scatter (arbitrary units; 0 μmol l^{-1} Ca^{2+}) (A) reveals a skewed population with low side-scatter, indicating heterogeneous small particles presumed to be vesicles of differing sizes. A plot of the number of events *versus* fluorescence (arbitrary units) (D) reveals a peak in fluorescence associated with these vesicles. The analysis that follows is from the larger vesicles (one-quarter of the distance along the *x* axis, as indicated by black bars projecting onto both the horizontal and vertical axes in B and F). Contour plots of fluorescence (logarithmic scale in arbitrary units) *versus* side-scatter (vesicle size in arbitrary units) are illustrated under control conditions (B, 0 μmol l^{-1} Ca^{2+}, 0 mmol l^{-1} ATP) and with the addition of 1 μmol l^{-1} Ca^{2+} alone (C, 0 mmol l^{-1} ATP), 5 mmol l^{-1} ATP alone (E, 0 μmol l^{-1} Ca^{2+}) and both Ca^{2+} and ATP (F).

Ca^{2+} in the presence of extravesicular ATP, confirming ATP-dependent Ca^{2+} uptake *via* PMCA.

Fluo-3 is deemed an appropriate fluorescent Ca^{2+} chelator because of its high affinity for Ca^{2+} (K_d, 396 nmol l^{-1}), its low autofluorescence (in the absence of Ca^{2+}), its broad response range and its ability to be excited with a low-power argon laser at 488 nm, thus enabling one to use a small benchtop instrument possessing fixed optical systems and limited options with regard to data analysis. Further, its emission at 526 nm provides for easy detection since this is within the visible wavelength range. As free [Ca^{2+}] increases, the emission intensity increases but remains at the same wavelength. We present preliminary results of the application of this technique to the study of Ca^{2+} uptake mechanisms in crayfish vesicles.

Basolateral membrane vesicles (BLMVs) were isolated from the hepatopancreas of individual intermoult crayfish using published techniques (Wheatly et al., 1998) and were preloaded with the fluorescent dye Fluo-3 (200 μmol l^{-1} pentapotassium salt, Molecular Probes) at the point in the procedure when resealing occurs. Vesicles were harvested and incubated with polyclonal antifluorescein antibodies (25 μg ml^{-1}) for 15 min to quench Fluo-3 fluorescence on the exterior of the vesicles and on cellular debris. The vesicles were pelleted by centrifugation and incubated for 30 min in intravesicular medium containing 100 mmol l^{-1} KCl, 5 mmol l^{-1} $MgCl_2$ and 25 mmol l^{-1} Hepes/Tris at pH 7.4 (at 4 °C). These vesicles were then repelleted and resuspended in extravesicular medium (the composition of which varied depending upon the experiment). They were then injected into the flow cytometer in a sheath buffer of extravesicular medium, which provided laminar flow. The vesicles passed the gated laser at a rate of 1000 s^{-1}, enabling statistical averaging of events. Ca^{2+} uptake/loss was measured as a change in fluorescence in response to experimental manipulation. Samples were analyzed on a Becton Dickinson FacScan (San Jose, CA, USA) for forward scatter and 90 ° side-scatter (linear scaling, *x* axis) and Fluo-3 green fluorescence (logarithmic scaling, *y* axis) by using a single 15 mW argon laser emitting at 488 nm. Data were analyzed using PC-LYSIS version 2 (Becton-Dickinson) and WinMDI version 1.3.3 software (Joseph Trotter, Salk Institute).

Initially, we tested the technique by determining the kinetics and associated pharmacology of intermoult PMCA, previously documented using the rapid filtration $^{45}Ca^{2+}$ uptake method (Wheatly et al., 1999). In these experiments, the extravesicular medium contained 25 mmol l^{-1} Hepes/Tris at pH 7.4, 100 mmol l^{-1} KCl, 0.5 mmol l^{-1} EGTA, 0.5 mmol l^{-1} HEEDTA, 0.5 mmol l^{-1} nitrilotriacetic acid, 5 mmol l^{-1} $MgCl_2$ (1.52 mmol l^{-1} free Mg^{2+}) and 0.72 mmol l^{-1} $CaCl_2$ (0–5 μmol l^{-1} free Ca^{2+}). The free Ca^{2+} and Mg^{2+} concentrations were calculated using the program *Chelator* (Schoenmakers et al., 1992). The first and second protonations of the ligands in the Ca^{2+} buffers (ATP, EGTA, HEEDTA, nitrilotriacetic acid) were taken into account, and the stability constants were adjusted in accordance with the pH, temperature and ionic strength of the medium. In 250 μl of reaction mixture, the reaction was begun by adding 5 μl of vesicles (equivalent to 6.6×10^{-4} mg of protein).

For each experimental condition, a mean fluorescence intensity (I_F) was determined. The ATP-dependent Ca^{2+} influx in the presence of added Ca^{2+} was expressed as the fold increase (*F*) in fluorescence intensity over background (ATP-dependent Ca^{2+} influx in the absence of added Ca^{2+}) using equations derived by Telford and Miller (1996):

$$F = \frac{I_F(+Ca^{2+}, +ATP) - I_F(+Ca^{2+}, -ATP)}{I_F(-Ca^{2+}, +ATP) - I_F(-Ca^{2+}, -ATP)} .$$

Fluorescence was measured following the addition of ATP (and compared with the value in the absence of ATP) for the following conditions: Ca^{2+}-dependence ([Ca^{2+}] varied from 0 to 5 μmol l^{-1}); the effect of 1 mmol l^{-1} NaN_3 and 5 μg ml^{-1} oligomycin B (together, they inhibit any residual mitochondrial ATPase activity); and the effect of vanadate, a non-specific inhibitor of phosphorylated ATPases.

Fig. 2 illustrates representative flow cytometry data for ATP-dependent Ca^{2+} uptake (*via* PMCA) into crayfish hepatopancreas BLMVs. A plot of the number of events *versus* 90 ° side-scatter (linear scaling, Fig. 2A) reveals a skewed population of events with low side-scatter, indicating heterogeneous particles (i.e. vesicles of differing sizes), as revealed in an earlier study by transmission electron microscopy (Wheatly et al., 1998). A plot of the number of events *versus* fluorescence (logarithmic scaling, Fig. 2D) reveals a peak in fluorescence associated with these vesicles. Initial analysis of the high-density but small vesicles (0–200 arbitrary units on the *x* axis linear scale in Fig. 2A) failed to produce intelligible data. However, analysis of the larger vesicles (200–400 arbitrary units on the linear scale, upper tail in Fig. 2A) revealed a sixfold increase in fluorescence resulting from ATP-dependent Ca^{2+} uptake. The simplest way to interpret these data is to select a point approximately one-quarter of the distance along the *x* axis of the four lower panels, which are contour plots of fluorescence (logarithmic scale) *versus* side-scatter (linear scale). In the absence of both Ca^{2+} and ATP (Fig. 2B), the average background fluorescence at the mid point of the plume is $10^{1.15}$. In the presence of either Ca^{2+} (Fig. 2C) or ATP (Fig. 2E), the fluorescence is unchanged. However, the addition of both Ca^{2+} and ATP (Fig. 2F) results in an increase in mean fluorescence to $10^{1.8}$.

Fluo-3 fluorescence was calibrated with free Ca^{2+} in the presence of 10 μg ml^{-1} of the Ca^{2+} ionophore A_{23187}. The 4.46-fold increase in fluorescence illustrated in Fig. 2 equates to an intravesicular free [Ca^{2+}] of 0.93 μmol l^{-1}. Uptake measured under identical experimental conditions using the rapid filtration technique with $^{45}Ca^{2+}$ at this [Ca^{2+}] corresponds with a flux rate of 20 pmol mg^{-1} min^{-1} (Wheatly et al., 1999). Using flow cytometry, we confirmed intermoult PMCA characteristics that closely resembled those determined using rapid filtration of $^{45}Ca^{2+}$-loaded vesicles. The increase in fluorescence exhibited [Ca^{2+}]-dependence; the K_m of 0.15 μmol l^{-1} showed strong agreement with the value determined using the rapid filtration technique (0.27 μmol l^{-1};

Wheatly et al., 1999). Inhibitors of residual mitochondrial ATPase activity (azide/oligomycin B) had no effect, suggesting that the vesicle preparation was minimally contaminated with mitochondria. Vanadate, a non-specific inhibitor of P-type ATPases, significantly inhibited Ca^{2+} influx, confirming an ATP-dependent Ca^{2+} uptake mechanism, presumed to be PMCA. On the basis of the correspondence with values obtained using the rapid filtration technique, flow cytometry would appear to be a promising new technique, especially since it can be performed on minimal amounts of material.

Novel molecular approaches

Background and obstacles for elusive moulting stages

Ca^{2+} pumps are integral membrane proteins containing approximately 1000 amino acid residues with three cytoplasmic domains (an ATP-binding site, a phosphorylation site and a transduction domain) joined to a set of 10 transmembrane α-helices by a narrow pentahelical stalk of α-helices (Wheatly and Zhang, 1999). We have cloned and sequenced the complete cDNA sequence of SERCA from crayfish axial abdominal muscle (Zhang et al., 2000; GenBank accession no. AF025849) and heart (D. D. Chen, Z. Zhang and M. G. Wheatly, unpublished data; GenBank accession no. AF025848) and have quantified tissue-specific expression throughout the moulting cycle. These two isoforms differ in their C-terminal region: the heart isoform possesses an extra 27 hydrophobic amino acid residues that may form an additional transmembrane domain. Southern analysis suggests that these two isoforms are encoded by a single gene. In addition, we have cloned and sequenced a 2764-base-pair partial PMCA cDNA that covers approximately 85 % of the coding sequence and appears to be ubiquitous. NCX1 is typically a protein of 970 amino acid residues consisting of 11 transmembrane regions (containing the ion-exchange functions) with a large hydrophilic loop between transmembrane segments 5 and 6 (the regulatory site; Nicoll et al., 1990). To date, we have cloned and sequenced an 858-base-pair partial cDNA from crayfish egg NCX that covers one-third of the predicted coding region.

We are interested in the cytochemical localization of these proteins in Ca^{2+}-transporting epithelia (such as gills/antennal gland/hepatopancreas/hypodermis) and non-Ca^{2+}-transporting tissues (such as muscle). Specifically, we want to determine the tissue distribution using bright-field/epifluorescence microscopy, the localization within cell types and the subcellular distribution (using confocal/electron microscopy) to elucidate their physiological roles. Antibodies would enable us to assess localization across and within transporting epithelia and to determine abundance (location/density) at different stages in the moulting cycle (correlated with differential transepithelial Ca^{2+} flux). We initially tried to use mammalian antibodies, but without success. For NCX, we had some success with the antibody to squid NCX kindly loaned by Dr Kenneth Philipson. However, in the long term, we felt it was critical to develop our own specific antibodies that could be employed for immunocytochemistry using light, electron and laser scanning confocal microscopy. In the present paper, we report the successful generation of antibodies to crayfish SERCA, PMCA and NCX, confirmed through hybridization with target tissues using bright-field microscopy.

Generation and characterization of polyclonal antibodies against crayfish SERCA, PMCA and NCX

Amino acid sequences deduced from cDNA sequences for crayfish SERCA, PMCA and NCX were used to design antigenic oligopeptides (14–15 amino acid residues plus cysteine at one end; Table 1) according to Boersma et al. (1993). A BLAST search of GenBank confirmed that the

Table 1. *Antigenic oligopeptides designed to generate antibodies against crayfish Ca^{2+} transporters*

Isoform	Antibody identity	Boost (weeks)	Oligopeptide antigen	Molecular location	ELISA[4] Optical density at 415 nm	Antiserum dilution
NCX1	213/214[1]	6	DYEAAEGELVFENNEC	Large intracellular loop between transmembrane segments 5 and 6	0.1–0.6	1:100 000
NCX2	223/224	6	EEGDDDEDEEGGEEC	,,	None	None
PMCA1	221/222	6	CAEINQVHFENEPN	Large cytoplasmic loop between FITC[2] and FSBA[3]	0.1–0.6	1:100 000
PMCA2	217/218	6	EGKEFNRRVRDESGC	,,	0.1–0.6	1:100 000
SERCA1	215/216	6, 10	QERNAESAIEALKEYC	Small cytoplasmic loop, cardiac and skeletal muscle isoforms	0.1	1:40 000
SERCA2	219/220	6, 10	CIARNYTDGENNLYK	C terminus, specific to heart isoform	0.1–0.5	1:100 000

[1]Two rabbits were used to raise antibody to each antigen.
[2]Fluorescein isothiocyanate site.
[3]5′-*p*-Fluorosulphonylbenzoyladenosine binding site.
[4]Enzyme-linked immunosorbent assay.
NCX, Na^+/Ca^{2+} exchanger; PMCA, plasma membrane Ca^{2+}-ATPase; SERCA, sarco/endoplasmic reticulum Ca^{2+}-ATPase.

sequences were unique. The designed oligopeptides were synthesized commercially (Genemed Biotech Inc, San Francisco, CA, USA). To increase antigenicity, they were conjugated to cationized bovine serum albumin (BSA, Pierce). The antigenic peptide cBSA conjugates were subsequently used to produce polyclonal antibodies in New Zealand White rabbits in compliance with LACUC protocol AUP 245 issued to Dr Harold Stills, WSU Veterinarian. Rabbits (2 kg) were obtained from a commercial rabbit supplier and were housed in the animal care facility at Wright State University, which operates under United States National Institutes of Health guidelines and has an Assurance of Compliance with the Public Health Service Policy on the Care and Use of Laboratory Animals. Trained staff performed all the injections, blood collections and euthanasia procedures.

Following the standard acclimation/quarantine period, each rabbit (two for each antigenic oligopeptide) was tranquillized (1 mg kg^{-1} Acepromazine, subcutaneously), and a 10 ml preimmune serum sample was collected from the central auricular artery and frozen (–80 °C). The back of each rabbit was then clipped and scrubbed with iodophor antiseptic (Betadine). Each rabbit was then injected intradermally at 20 sites with 0.5 ml of the antigen/Freund's complete adjuvant mixture (100–500 µg of immunogen) using aseptic procedures. At 4 and 6 weeks post-injection and weekly thereafter, each rabbit was tranquillized with 0.5 mg kg^{-1} Acepromazine subcutaneously, and a 10 ml blood sample was removed from the central auricular artery and used to monitor primary antibody titre by enzyme-linked immunosorbent assay (ELISA).

Antibody titre was tested by ELISA using the synthetic peptide as antigen. ELISA plate wells were coated with 100 µl of antigenic oligopeptide (2 µg ml^{-1} in phosphate-buffered saline, PBS, per well). Negative controls included 100 µl of non-specific oligopeptide (2 µg ml^{-1} in PBS) per well and wells filled with 100 µl of PBS without antigen. The samples were incubated at 37 °C for 4 h. After four washes with phosphate-buffered saline Tween (PBST), the samples were blotted overnight at 37 °C. Primary antibody was applied to the wells

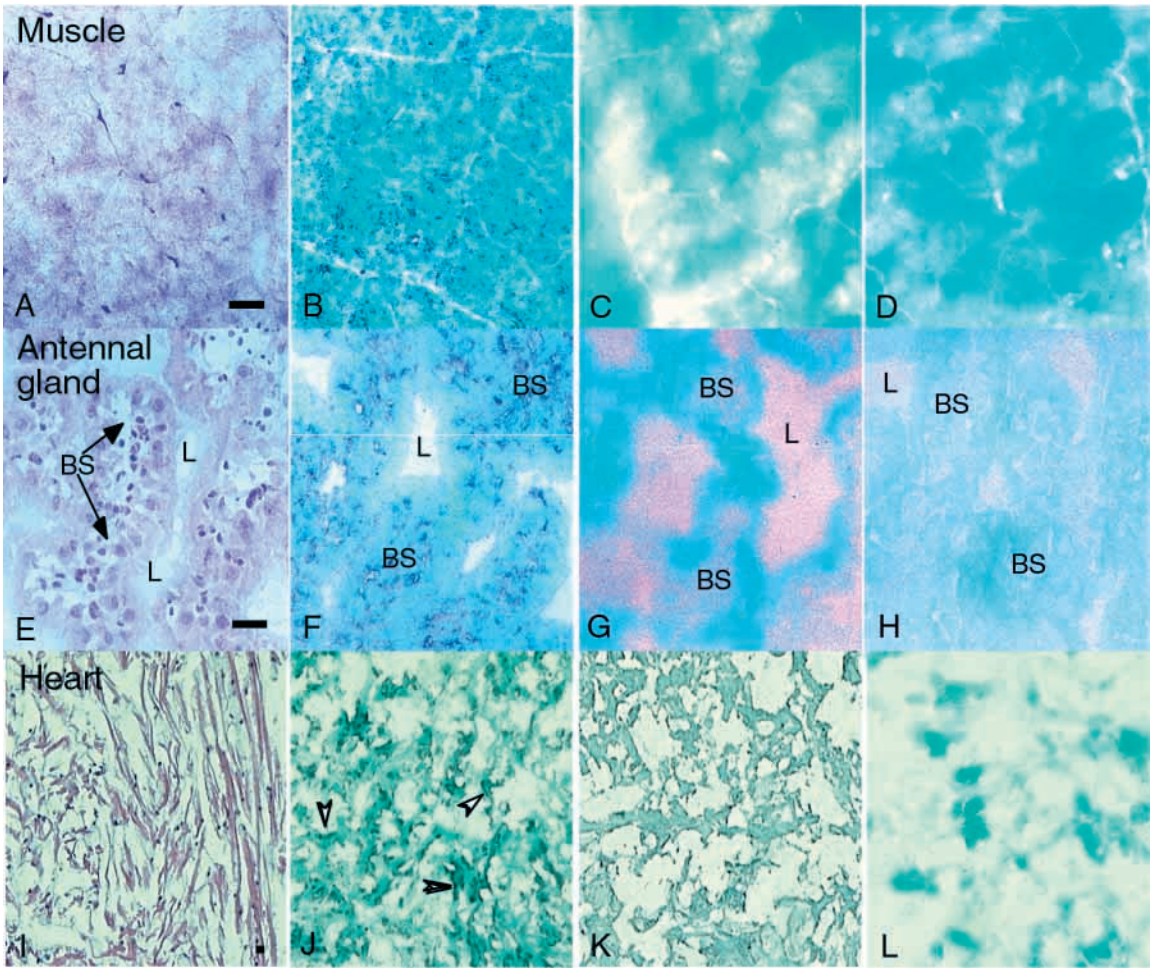

Fig. 3. Immunocytochemistry of intermoult crayfish tissues. From the top: SERCA1, sarco/endoplasmic reticulum Ca^{2+}-ATPase (antibody 215) in axial abdominal muscle (A–D); PMCA1, plasma membrane Ca^{2+}-ATPase (antibody 221) in antennal gland (E–H); NCX1, Na^{+}/Ca^{2+} exchanger (antibody 213) in cardiac muscle (I–L). From the left: haematoxylin and eosin stain for general structure (A,E,I); primary antibody (B,F,J); negative control, preimmune serum (C,G,K); and negative control, in the absence of primary antibody (D,H,L). Scale bar, 25 µm. BS, blood space, L, lumen. Arrowheads indicate regions of dark staining.

as triplets with serial dilutions in PBST-BSA for 2 h at 37 °C. The wells were then washed four times with PBST. Secondary antibody, goat anti-rabbit IgG conjugated with horseradish peroxidase (500 μg ml^{-1}), was diluted 1:3000 with PBS, and a sample of it (100 μl) was applied to each well. The plates were incubated at 37 °C for 2 h. The plates were washed four times. A mixture of peroxidase substrate [2,2′-azino-di-(3-ethylbenzthiazoline-6-sulphonic acid) and hydrogen peroxide; Bio-Rad] was prepared immediately before use, and 100 μl of the solution was added to each well. The contents of the well were mixed with gentle shaking. Greenish-blue colour development took place at room temperature (21 °C) for approximately 20 min. Stop solution (0.2 % oxalic acid) was added to each sample. The plates were read at 415 nm using a Spectra MAX 250 plate reader (Molecular Devices).

All rabbits were boosted at 6 weeks after the initial inoculation. Two weeks later, six rabbits with an adequate antibody response (Table 1) were killed (PMCA1, PMCA2, NCX1). The NCX2 antigen, however, failed to elicit an immune response, and those two rabbits were removed from the study. The remaining four rabbits were booster-injected again at 10 weeks after the initial injection and killed at 12 weeks (SERCA1, SERCA2). Rabbits were deeply anaesthetized with 40 mg kg^{-1} of sodium pentobarbital intravenously and terminally exsanguinated by cardiac venipuncture using an 18 gauge needle. They were eventually killed by intravenous pentobarbital injection (100 mg kg^{-1}).

The specificity of each antiserum was confirmed in a target tissue selected on the basis of high abundance of the Ca^{2+} transporter documented through northern analysis. Axial abdominal muscle was selected for SERCA because of the prominent role in Ca^{2+} resequestration following muscle relaxation. Antennal gland was selected for PMCA because of renal reabsorption of 97 % of filtered Ca^{2+}. Cardiac muscle was selected for NCX because of documented high abundance and vigorous activity. We then employed immunocytochemical localization using bright-field light microscopy. The protocol selected employs permanent colorimetric visualization on frozen sections (preserves antigenicity) and was modified from published methods on other exchangers and pumps (Kimura et al., 1994, Na^+/H^+ exchanger in lobster; Zhuang et al., 1999, V-type H^+-ATPase in mosquito midgut; Sullivan et al., 1995, H^+-ATPase in trout gill).

Tissues of interest were dissected, immersed and embedded in OCT compound (Tissue-Tek), and then frozen rapidly in isopentane cooled with liquid N_2 and stored at −70 °C. Frozen sections (6–8 μm) were cut on a cryostat at −22 °C, collected on positively charged slides, air-dried (4 h), fixed in acetone (15 min) and stored at −70 °C. Sections were rinsed (in TBS), and then incubated with 1% BSA in TBS and then goat blocking serum. Sections were then incubated overnight at 4 °C with the primary polyclonal rabbit antibody to SERCA, PMCA or NCX (final primary antibody concentration was 20 mg ml^{-1} diluted in PBS) diluted in Tris buffer containing 0.3 % Triton X-100 (TCT, to permeabilize cells to gain access to intracellular epitopes). Negative controls aimed at demonstrating that the staining pattern was specific to the transporter of interest included (i) incubation with preimmune serum and (ii) complete omission of primary antibody. Primary antibody binding was visualized using biotinylated goat anti-rabbit IgG secondary antibody (30 min) at room temperature (21 °C) from the ImmunoPure ABC alkaline phosphatase staining kit, generating a black substrate (Pierce, Rockford, IL, USA). Sections were subsequently counterstained in 1 % Fast Green (30 s) to allow visualization of cellular structure. Sections were then dehydrated, cleared in xylene and mounted for viewing on a Nikon labophot microsope.

As shown on Fig. 3, the three antibodies tested to date show specific binding (darkly stained regions, panels second from the left) compared with negative controls (two right-hand panels). Comparison with sections stained with haematoxylin and eosin (far left) confirm specific locations within cells. As predicted, SERCA was associated with the sarcoplasmic reticulum. PMCA was associated with basolateral membranes facing the blood space and was absent from the apical (luminal) membrane. NCX was located on the periphery of cardiac cells. This is excellent preliminary evidence that the antibodies can be used for localization studies.

Jean-Paul Truchot's papers on acid–base balance and respiration in crustaceans are some of the best thumbed in my (M.G.W.) reprint collection! My early interest in decapods relied heavily on his original research in the 1970s and 1980s, and I thank him for providing the opportunity to keep up my 'O-level' French! The research outlined in this review was funded by NSF grants IBN 9307290, 9603723 and 9870374. We thank Dr William Telford for assisting us with the flow cytometry work and the Department of Microbiology and Immunology at WSU for allowing us access to the flow cytometer. The antisera described in this article are available to the scientific community upon written request to M.G.W.

References

Ahearn, G. A. and Franco, P. (1993). Ca transport pathways in brush border membrane vesicles of crustacean antennal glands. *Am. J. Physiol.* **264**, R1206–R1213.

Ahearn, G. A. and Zhuang, Z. (1996). Cellular mechanisms of calcium transport in crustaceans. *Physiol. Zool.* **69**, 383–402.

Boersma, W. J. A., Haaijman, J. J. and Claassen, E. (1993). Use of synthetic peptide determinants for the production of antibodies. In *Immunohistochemistry*, vol. II (ed. A. C. Cuello), pp. 1–78. New York: Wiley.

Cameron, J. N. and Wood, C. M. (1985). Apparent H^+ excretion and CO_2 dynamics accompanying carapace mineralization in the blue crab (*Callinectes sapidus*) following moulting. *J. Exp. Biol.* **114**, 181–196.

Flik, G., Verbost, P. M., Atsma, W. and Lucu, C. (1994). Calcium transport in gill plasma membranes of the crab *Carcinus maenas*: evidence for carriers driven by ATP and a Na^+ gradient. *J. Exp. Biol.* **195**, 109–122.

Greenaway, P., Dillaman, R. M. and Roer, R. D. (1995). Quercetin-dependent ATPase activity in the hypodermal tissue of *Callinectes*

sapidus during the moult cycle. *Comp. Biochem. Physiol.* **111**, 303–312.

Ishida, Y. and Chused, T. M. (1988). Heterogeneity of lymphocyte calcium metabolism is caused by T cell-specific calcium sensitive potassium channel and sensitivity of the calcium ATPase pump to membrane potential. *J. Exp. Med.* **168**, 839–852.

Kimura, C., Ahearn, G. A., Busquets-Turner, L., Haley, S. R., Nagao, C. and De Couet, G. (1994). Immunolocalization of an antigen associated with the invertebrate electrogenic $2Na^+/1H^+$ antiporter. *J. Exp. Biol.* **189**, 85–104.

Klein, M. J. and Ahearn, G. A. (1999). Calcium transport mechanisms of crustacean hepatopancreatic mitochondria. *J. Exp. Zool.* **283**, 147–159.

Mangum, C. P., de Fur, P. L., Fields, J. H. A., Henry, R. P., Kormanik, G. A., McMahon, B. R., Ricci, J., Towle, D. W. and Wheatly, M. G. (1985). Physiology of the blue crab *Callinectes sapidus* Rathbun during a moult. In *National Symposium on the Soft-shelled Blue Crab Fishery* (ed. H. M. Perry and R. F. Malone) pp. 1–12. Biloxi: Gulf Coast Research Laboratory.

McMahon, B. R. and Wilkens, J. (1983). Ventilation, perfusion and oxygen uptake. In *The Biology of Crustacea*, vol. 5 (ed. L. H. Mantel and D. E. Bliss), pp. 289–372. London, New York: Academic Press.

Nicoll, D. A., Longini, S. and Philipson, K. D. (1990). Molecular cloning and functional expression of the cardiac sarcolemmal Na^+–Ca^{2+} exchanger. *Science* **250**, 562–565.

Rogers, J. V. and Wheatly, M. G. (1997). Accumulation of calcium in the antennal gland during the moulting cycle of the freshwater crayfish *Procambarus clarkii*. *Invert. Biol.* **116**, 248–254.

Schoenmakers, T., Visser, G. J., Flik, G. and Theuvenet, A. P. R. (1992). Chelator: an improved method for computing metal ion concentrations in physiological solutions. *Biotechniques* **12**, 870–879.

Sullivan, G. V., Fryer, J. N. and Perry, S. F. (1995). Immunolocalization of proton pumps (H^+-ATPase) in pavement cells of rainbow trout gill. *J. Exp. Biol.* **198**, 2619–2629.

Telford, W. G. and Miller, R. A. (1996). Detection of plasma membrane Ca^{2+} ATPase activity in mouse T lymphocytes by flow cytometry using fluo-3-loaded vesicles. *Cytometry* **24**, 243–250.

Truchot, J. (1983). Regulation of acid–base balance. In *The Biology of Crustacea*, vol. 5 (ed. L. H. Mantel and D. E. Bliss), pp. 431–457. London, New York: Academic Press.

Wheatly, M. G. (1996). An overview of calcium balance in crustaceans. *Physiol. Zool.* **69**, 351–382.

Wheatly, M. G. (1997). Crustacean models for studying calcium transport: the journey from whole organisms to molecular mechanisms. *J. Mar. Biol. Ass. UK* **77**, 107–125.

Wheatly, M. G. (1999). Calcium homeostasis in Crustacea: the evolving role of branchial, renal, digestive and hypodermal epithelia. *J. Exp. Zool.* **283**, 620–640.

Wheatly, M. G. and Hart, M. K. (1995). Hemolymph ecdysone and electrolytes during the moulting cycle of crayfish: a comparison of natural moults with those induced by eyestalk removal or multiple limb autotomy. *Physiol. Zool.* **68**, 583–607.

Wheatly, M. G., Pence, R. C. and Weil, J. R. (1999). ATP-dependent calcium uptake into basolateral vesicles from transporting epithelia of intermoult crayfish. *Am. J. Physiol.* **276**, R566–R574.

Wheatly, M. G., Weil, J. R. and Douglas, P. B. (1998). Isolation, visualization, characterization and osmotic reactivity of crayfish BLMV. *Am. J. Physiol.* **274**, R725–R734.

Wheatly, M. G. and Zhang, Z. (1999). Physiological and molecular characterization of the calcium pump: evolutionary considerations. In *Calcium Metabolism: Comparative Endocrinology* (ed. J. Danks, C. Dacke, G. Flik and C. Gay) pp. 13–20. Bristol: BioScientifica Ltd.

Zhang, Z., Chen, D. and Wheatly, M. G. (2000). Cloning and characterization of sarco/endoplasmic reticulum Ca^{2+}-ATPase (SERCA) from crayfish axial muscle. *J. Exp. Biol.* **203**, 3411–3423.

Zhuang, Z. and Ahearn, G. A. (1996). Ca^{2+} transport processes of lobster hepatopancreas brush border membrane vesicles. *J. Exp. Biol.* **199**, 1195–1208.

Zhuang, Z. and Ahearn, G. A. (1998). Energized Ca^{2+} transport by hepatopancreatic basolateral plasma membranes of *Homarus americanus*. *J. Exp. Biol.* **201**, 211–220.

Zhuang, Z., Linser, P. J. and Harvey, W. R. (1999). Antibody to H^+ V-ATPase subunit E colocalizes with portasomes in alkaline larval midgut of a freshwater mosquito (*Aedes aegypti* L.). *J. Exp. Biol.* **202**, 2449–2460.